IEEE Access
Multidisciplinary ⋮ Rapid Review ⋮ Open Access Journal

Received December 17, 2019, accepted December 28, 2019, date of publication January 3, 2020, date of current version January 10, 2020.

Digital Object Identifier 10.1109/ACCESS.2019.2963680

A Linear Piezoelectric Stick-Slip Actuator via Triangular Displacement Amplification Mechanism

XIAOHUI LU[1], QIANG GAO[1], YIKANG LI[1], YANG YU[1], XIAOSONG ZHANG[1], GUANGDA QIAO[1], AND TINGHAI CHENG[1,2]

[1]School of Mechatronic Engineering, Changchun University of Technology, Changchun 130012, China
[2]Beijing Institute of Nanoenergy and Nanosystems, Chinese Academy of Sciences, Beijing 100083, China

Corresponding author: Tinghai Cheng (chengtinghai@163.com)

This work was supported in part by the Technology Research Planning Project of Education Department of Jilin Province under Grant JJKH20181037KJ and Grant JJKH20191293KJ, in part by the Project of Industrial Technology Research and Development of Jilin Province Development and Reform Commission under Grant 2019C037-6, and in part by the Science and Technology Development Plan of Jilin Province under Grant 20190201108JC.

ABSTRACT In the field of piezoelectric actuators, high speed piezoelectric stick-slip actuators have received considerable attention. A linear stick-slip piezoelectric actuator is proposed in this article, which combines asymmetric flexure hinge with triangular displacement amplification mechanism. The designed linear piezoelectric stick-slip actuator can achieve high speed at lower frequency. The configuration of the actuator and driving principle are illustrated and designed by theory and simulation. In order to study its performance, a prototype is fabricated, and an experimental system is established. The experimental results confirm that the maximum step efficiency of the prototype is 97.9 %. The maximum speed is 20.17 mm/s under the driving voltage of 100 V_{P-P}, the driving frequency of 610 Hz and the locking force of 2.5 N. The maximum load capacity is 2.4 N under the locking force of 3.5 N. The proposed piezoelectric stick-slip actuator increases the step efficiency and improves the output speed at lower frequency.

INDEX TERMS High speed, stick-slip actuators, asymmetric flexure hinge, triangular displacement amplification mechanism.

I. INTRODUCTION

Piezoelectric actuators play an important role in manufacturing [1], which are widely used in semiconductor manufacturing, biomedical manipulations [2], [3], microscope scanning [4], [5] and material micromechanical testing [6] due to their simple structure, fast response, large stroke and no electromagnetic interference [7]–[9]. They can be classified into four types according to the driving principles: direct-push[10], inchworm [11], [12], ultrasonic [13], [14] and stick-slip actuators [15]. The direct-push type actuators have high positioning accuracy and a large force [16], [17]. Inchworm type actuators can generate a large driving force [18], [19]. Ultrasonic type actuators require signals of higher frequencies to excite piezoelectric elements and achieve high speed [20]–[23]. Stick-slip type actuators have a simple structure and achieve a large work range [24], [25]. Its driving principle is that using the alternating change of static friction force and kinetic friction force between the stator and the slider push the slider to move. In the slow estension stage of the piezoelectric stack, the static friction force is generated, and the stator pushes the slider to advance a small displacement. The kinetic friction force is generated which is resistance during the quick contraction stage of the piezoelectric stack, making the slider produce a small backward motion [26]–[28].

With the rapid development in the field of machining and manufacturing, in order to improve manufacturing efficiency, the output speed of the piezoelectric stick-slip actuator is becoming more and more important. Therefore, it is crucial to develop a piezoelectric stick-slip actuator with high speed. In order to improve the output speed of the piezoelectric actuator, it is often used to increase the displacement of one step, the driving voltage, the driving frequency and reduce the backward motion. At present, research scholars have developed varieties of prototypes for different methods. Wei et al.

The associate editor coordinating the review of this manuscript and approving it for publication was Yingxiang Liu.

developed a compliant mechanism-based stepping motion actuator with multi-mode [29]. By increasing the driving voltage and frequency, Wang *et al.* developed a piezoelectric actuator using the parasitic motion idea combined with displacement amplification mechanism [30]. Zhang *et al.* realized the high speed of the piezoelectric stick-slip actuator by increasing the driving frequency [31], [32]. Zhong *et al.* developed an inertial stick-slip driving platform in combination with a flexible hinge mechanism [33]. Zhang *et al.* studied an anisotropic friction surface to reduce the backward motion [34]. In the previous study, Li *et al.* developed a bidirectional piezoelectric stick-slip actuator based on the principle of flexible hinge lever amplification [35], increasing the displacement of one step and the speed of the slider. And introduced ultrasonic vibration into the quick contraction stage of the piezoelectric stick-slip actuator and reduced the backward displacement of the actuator by using the ultrasonic anti-friction effect [36], which increased the output speed of the actuator. Guo *et al.* developed a piezoelectric stick-slip actuator with a higher speed at a lower frequency [37]. Various structures and methods are used to design the piezoelectric stick-slip actuator. The current piezoelectric stick-slip actuator mainly increases the output speed by increasing the driving frequency. However the structures of them are complex, and the sawtooth waveform of higher frequency will affect the lifetime of the actuators, and the piezoelectric stack excited by high frequency and high voltage will increase its heat. Therefore, it is very meaningful to propose a kind of simple structure piezoelectric stick-slip actuator with high speed at a lower frequency.

The actuator proposed by the article is based on asymmetric flexure hinge mechanism with triangular displacement amplification mechanism, which has the characteristics of large lateral displacement. And it greatly improves the output speed of the piezoelectric actuator at lower frequency. In addition, Section 2 introduces the driving principle of piezoelectric actuators. Section 3 conducts the finite-element method (FEM) and a theoretical analysis of the mechanism. Section 4 and 5 set up an experimental test system and analyze the performance of the actuator, respectively. Simulation verification, theoretical analysis, and experimental results show that the linear actuator has high speed and output efficiency, which expands its application in machining and manufacturing.

II. CONFIGURATION AND DRIVING PRINCIPLE

Figure 1 illustrates the driving process of the proposed prototype when the sawtooth wave signal is applied to the piezoelectric stack, and it can be divided into three stages in a sawtooth wave signal cycle. The driving voltage is shown in figure 1 (a). At time t_0, as shown in figure 1 (b), the slider is in the initial position and remains stationary. The locking force between the tip of the driving foot and the slider can be changed. From t_0 to t_1, as shown in figure 1 (c), the piezoelectric stack extends slowly with the excitation of sawtooth wave, and triangular displacement amplification

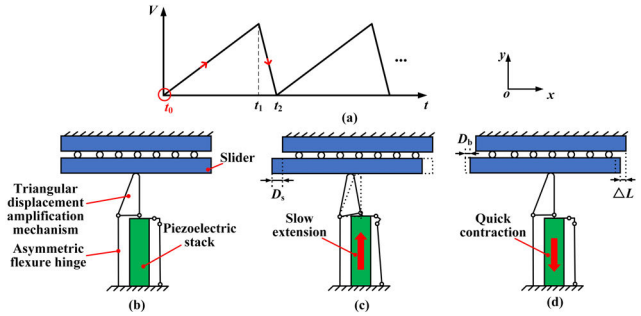

FIGURE 1. Driving principle. (a) Driving signal. (b) Initial state. (c) Slow extension stage. (d) Quick contraction stage.

TABLE 1. Simulation parameter values.

Simulation parameters	Parameter values
Density	2810 kg/m^3
Young's modulus	7.17×10^4 MPa
Poisson's ratio	0.33

mechanism is pushed by the piezoelectric stack. During this stage, the driving foot generates a displacement along the negative direction of the x-axis and the positive direction along the y-axis due to the deformation of the asymmetric flexure hinge. The friction force between the driving foot and the slider is the static friction force, which makes the slider move a small displacement D_s in the negative direction along the x-axis. From t_1 to t_2, as shown in figure 1 (d), the piezoelectric stack contracts quickly to its initial position. During this stage, the driving foot moves rapidly in the positive direction of x-axis and the negative direction of y-axis due to elastic deformation of flexure hinge. At the same time, the normal pressure decreases, and kinetic friction force is generated between the driving foot and the slider. And the slider causes a backward displacement D_b. The slider can move forward continuously by applying a continuous sawtooth wave to the piezoelectric stack. And the slider of the piezoelectric actuator moves $\Delta L = D_s - D_b$ in one signal cycle.

III. DESIGN AND SIMULATION ANALYSIS

In order to determine the structural parameters of triangular displacement amplification mechanism. FEM software is used to carry out static structural simulation analysis of triangular displacement amplification mechanism. The simulation material is AL7075, and the parameters corresponding to the simulation are shown in table 1:

During the FEM process, the fixed supports are applied to the two holes, and the internal surface of the upper side of the stator is pushed by 10 μm, as shown in figure 2. The simulated synthetic displacement of driving foot P is calculated by the following equation:

$$U_{sum} = \sqrt{U_x^2 + U_y^2} \tag{1}$$

U_x is the forward displacement along the x-axis, and U_y is the forward displacement along the y-axis of point P. Figure 2 shows the simulation results of structural statics.

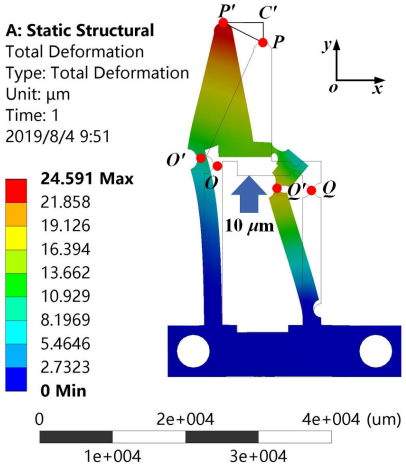

FIGURE 2. Structure static simulation diagram.

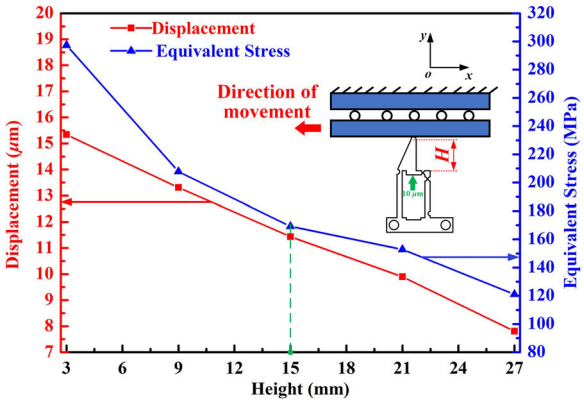

FIGURE 3. FEM curve of triangular displacement amplification mechanism.

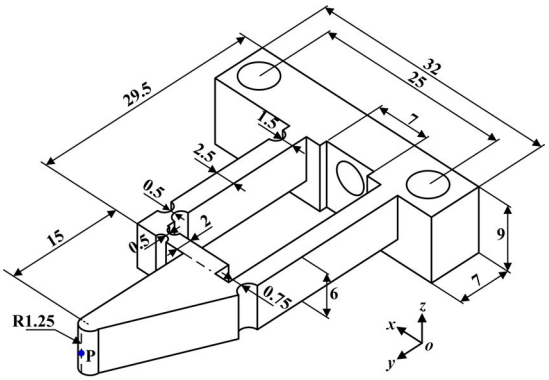

FIGURE 4. Main structural parameters of the stator (unit: mm).

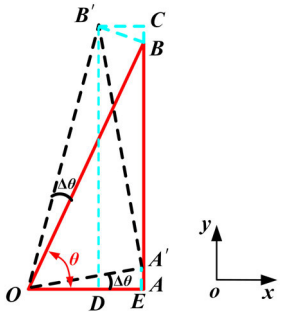

FIGURE 5. Schematic diagram of the triangular amplification mechanism.

TABLE 2. The values of the theoretical parameters.

Parameters	Values
OA	7.125 mm
AB	15.000 mm
OB	17.740 mm
$A'E$	10.000 μm
θ	66.324°

The simulation results show that the maximum displacement of point P along the x-axis is 25.34 μm, and the maximum equivalent stress is 67.1 MPa at the point Q', and it is less than the allowable stress 505 MPa of the material.

PC' is the displacement of point P along the y-axis. $C'P'$ is the displacement of point P along the x-axis. PP' is the synthetic displacement. The simulation results show that PC' equals U_y for 10.55 μm, and $C'P'$ equals U_x for 22.12 μm, PP' equals U_{sum} for 24.48 μm.

According to the design requirements, the key dimension H of the triangular displacement amplification mechanism is simulated and optimized. Figure 3 shows the performance analysis of stator's driving action on the slider under different H sizes. H is the distance between the bottom of the triangular displacement amplification mechanism and the center of the driving foot. This article mainly simulates the displacement of the slider along the x-axis and the equivalent stress of the driving foot. The analysis results show that with the increasing of H size, the displacement along the x-axis of the slider and the equivalent stress of the driving foot decrease. It can be seen from the simulation that the value of H affects lateral displacement, stiffness and structural compactness. Larger lateral displacements can increase the output speed, and less stress reduces wear of driving foot. In order to obtain a large lateral displacement, small stress and structural compactness of the prototype, this article H is selected as 15 mm and the value is the design size of the triangular displacement amplification mechanism.

The article dimensions the size of the stator, combining with the simulation analysis and the piezoelectric stack. As shown in figure 3, the triangular displacement amplification mechanism is optimized. And the size of flexure mechanism is limited by piezoelectric stack. Figure 4 shows the size parameters of a stator combining asymmetric flexure hinge and triangular displacement amplification mechanism.

Figure 5 shows a schematic diagram of the triangular displacement amplification mechanism which rotates counterclockwise around the point O. According to figure 4, the parameter values in figure 5 are obtained, and they are shown in table 2.

ΔOAB rotates $\Delta\theta$ angle around the point O (OA to OA', OB to OB', AB to $A'B'$) pushed by the piezoelectric stack, and $\Delta\theta$ can be calculated by the following equation:

$$\Delta\theta = \arcsin\frac{A'E}{OA'} \tag{2}$$

TABLE 3. Comparison of simulation and the oretical calculation data.

Simulation data		Theoretical data	
Simulation parameter	Simulation values (μm)	Calculating parameter	Calculated value (μm)
$C'P'$ (U_x)	-22.12	CB'	-24.06
PC' (U_y)	10.55	BC	6.82
PP'(U_{sum})	24.48	BB'	25.01

The lengths of BC and CB' are equal to the displacement of B to B' along the y-axis and the x-axis. The length of $B'D$ is equal to AC, so the length of $B'D$ can be calculated by the following equation:

$$B'D = OB' \times \sin(\theta + \Delta\theta) \tag{3}$$

The lengths of BC can be calculated by the following equation:

$$BC = OB' \times \sin(\theta + \Delta\theta) - AB \tag{4}$$

According to the motion property of a rigid body, the length of line segment OD:

$$OD = OB' \times \cos(\theta + \Delta\theta) \tag{5}$$

Since CB'= AD = OA-OD, the distance CB' can be obtained from equations (2) and (5), which can be expressed as follows:

$$CB' = OA - OB' \times \cos\left(\theta + \arcsin\frac{A'E}{OA'}\right) \tag{6}$$

Substitute the design parameters into equation (4) and equation (6), and the lengths of BC and $B'C$ can be calculated:

$$BC = 6.82\mu\text{m}, \quad CB' = 24.06\mu\text{m}.$$

The feasibility of the triangle amplification principle is verified within the allowable error range by comparing the simulation data with the theoretical data. Table 3 is the comparison table of simulation and theoretical calculation data. It can be seen from figure 2, in the actual process, the O point will move a small displacement. So there are slight errors between simulation and theoretical calculation verification.

IV. EXPERIMENTS

To verify the performance of the proposed actuator, an experimental system is established and a series of experiments are carried out to test output performances, such as output speed, load capacity and efficiency.

A. EXPERIMENTAL SYSTEM

As show in figure 6, an experimental system is constructed according to the test performance requirements of the experimental prototype. The experimental system mainly includes: a waveform generator (DG4162, Beijing RIGOL Technology Co. Ltd., China), a power amplifier (XE500-C, Harbin Core Tomorrow Science & Technology Co. Ltd., China), a prototype, a laser displacement sensor (LK-H020, Keyence Co. Ltd., Japan), a power analyzer

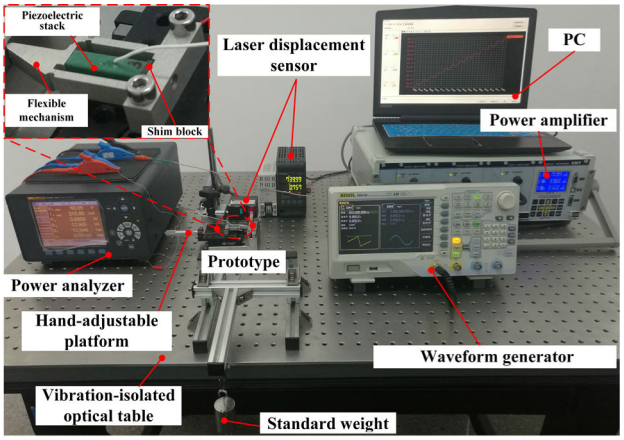

FIGURE 6. Photograph of the experimental system.

(NORMA 4000, FLUKE Co. Ltd., U.S), a vibration-isolated optical table, a personal computer. The prototype includes a base, a slider (VR3-75, THK), a hand-adjustable platform and a stator. The stator comprises a flexible mechanism which is made of AL7075 aluminum alloy, a piezoelectric stack (AE0505D16F, 5 mm × 5 mm × 20 mm, Tokin), a shim block and a screw. The flexible mechanism includes triangular displacement amplification mechanism and asymmetric flexure hinge mechanism. The preload force of piezoelectric stack is changed by adjusting the screw. The stator is fixed on the hand-adjustable platform by hexagonal screw. And the stator is manufactured by wire-electrical-discharge. The hand-adjustable platform is fixed on the base. The locking force between the driving foot of the stator and the slider is changed by adjusting the hand-adjustable platform. The weight of the slider is 35 g, and the output performance of the linear actuator is verified through experiment.

The waveform generator generates the driving signal, which is amplified by the power amplifier and sent to the piezoelectric stack, and pushes the slider to move. The laser displacement sensor collects the speed and displacement signal, and the power analyzer is used to calculate the input power. A weight is hanged on the fixed pulley through the steel wire, and the other end of the steel wire is connected to the end of the slider. In this way, the locking force of the experimental prototype is adjusted, and the load performance of the prototype is tested by changing the weight mass.

In addition, the natural frequency of the prototype is tested by a precision impedance analyzer (6500B, Wayne Kerr Electronics), as shown in figure 7. It can be concluded that the first-order natural frequency of the prototype is about 583.4 Hz from the impedance curve.

B. EXPERIMENTAL RESULT

In order to further verify the feasibility of the displacement amplification principle proposed by the article, the article conducted a series of performance tests on the processed prototype.

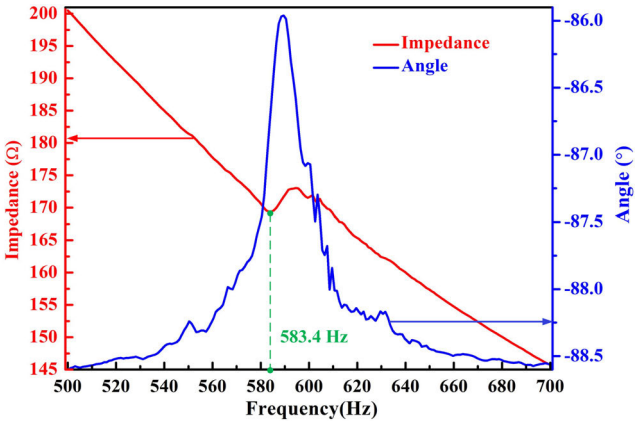

FIGURE 7. Impedance test curve of the prototype.

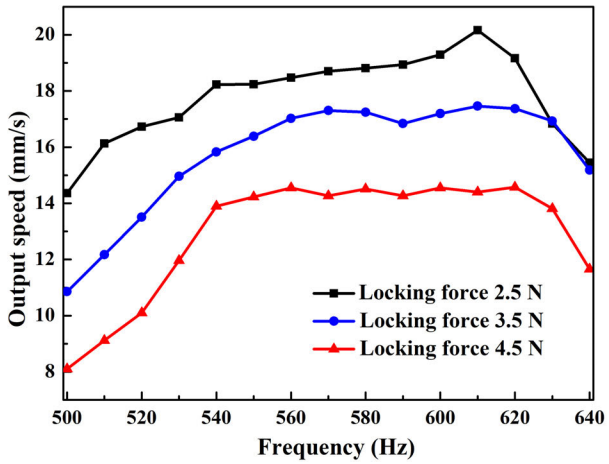

FIGURE 8. Relationship between the output speed and the driving frequency.

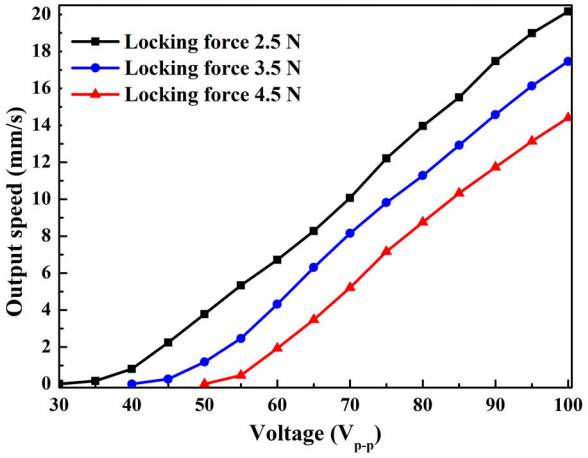

FIGURE 9. Relationship between the output speed and the driving voltage.

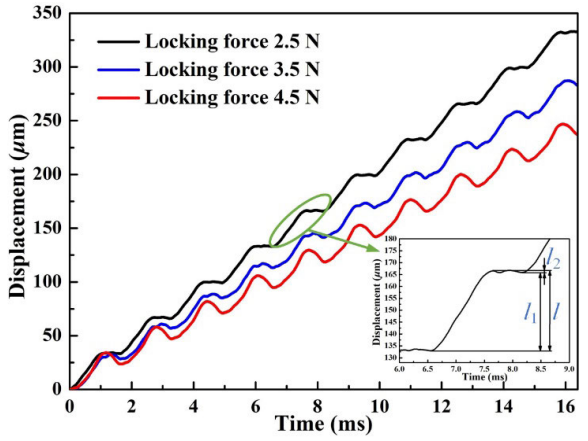

FIGURE 10. Relationship between the displacement and the time.

Figure 8 shows the relationship between the output speed and the drive frequency. As the driving frequency of the prototype increases from 500 Hz to 640 Hz, the output speed of the slider is tested under the driving voltage of 100 V_{P-P}, the duty ratio of 90 % and the locking force of 2.5 N, 3.5 N and 4.5 N, respectively. It can be seen from the experimental curve that as the driving frequency increases, the output speeds of the slider increases and then decreases. When the driving frequency reaches 610 Hz, the output speed of the prototype peaks at the locking force of 2.5 N, 3.5 N, and it is 20.17 mm/s and 17.46 mm/s, respectively. When the driving frequency reaches 610 Hz, the speed of the prototype is 14.4 mm/s at the locking force of 4.5 N. And when the driving frequency reaches 620 Hz, the speed of the prototype peaks and it is 14.58 mm/s when the locking force is 4.5 N. Therefore, the optimum frequency for the best performance of the prototype is 610 Hz.

Figure 9 shows the relationship between the output speed of the slider and the driving voltage when the sawtooth driving frequency is 610 Hz. It can be seen from the experimental data that the speed of the prototype increases linearly with the increasing of the driving voltage. When the driving voltage is 100 V_{P-P}, the duty ratio of 90 % and the locking forces are 2.5 N, 3.5 N, and 4.5 N, the speeds of the slider are 20.17 mm/s, 17.46 mm/s and 14.4 mm/s, respectively. Therefore, the maximum output speed of the slider is 20.17 mm/s when driving frequency is 610 Hz and the locking force is 2.5 N, and the minimum starting voltage of the prototype is 30.15 V_{P-P}.

Figure 10 shows the relationship between the displacement and the time of the slider under different locking forces. The backward motion can be observed in every step. When the piezoelectric stack looses power quickly, the friction force between the slider and the driving foot changes to be the kinetic friction force and it changes the motion direction. Thus, the slider will move back a small distance. The proposed actuator has smaller backward motion than the previous work [38]. Therefore, compared with the existing piezoelectric stick-slip actuators, it can have a higher speed at a lower frequency. It should be noted that the backward motion increases when the locking force increases.

Under the locking force of 2.5 N, the driving frequency of 610 Hz, the driving voltage of 100 V_{P-P}, the real step

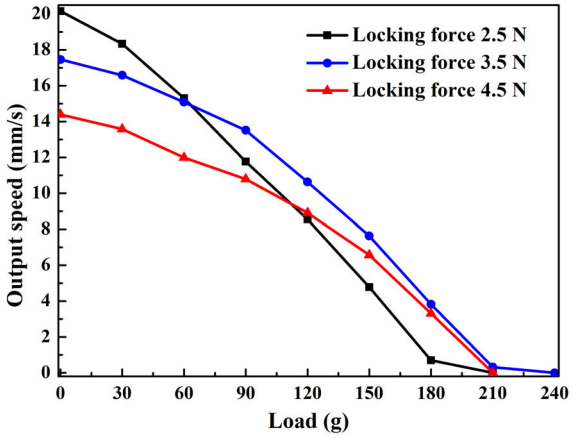

FIGURE 11. Relationship between the output speed and the load.

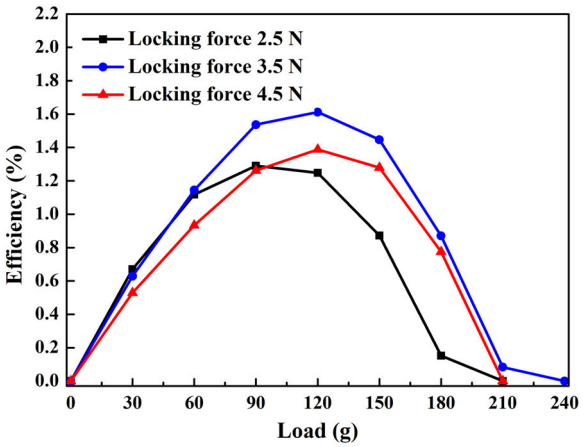

FIGURE 12. Relationship between the efficiency and the load.

displacement l_1 of the slider is the largest and the step efficiency is the highest. The step efficiency can be obtained by the following equation:

$$\eta_0 = \frac{l_1}{l} \times 100\% = \frac{l - l_2}{l} \times 100\% \tag{7}$$

Among them, is the step efficiency of the prototype. l_1 is the real step displacement and it is 32.89 μm. l is the maximum displacement of one step and it is 33.59 μm. l_2 is the backward displacement of one step. The maximum step efficiency is 97.9 %.

Figure 11 shows the relationship between the output speed and load under different locking forces. The case that the slider is pushed only by stator is regarded as an unloaded condition, and the mass of the slider is about 35 g. It can be seen from the figure 11, as the load increases, the output speed of the slider decreases. Under the locking forces of 2.5 N, 3.5 N and 4.5 N, driving voltage of 100 V_{P-P} and the duty ratio of 90 %, the maximum load is 2.1 N, 2.4 N, 2.1 N, respectively.

The efficiency of the piezoelectric stick-slip actuator is an important performance. And it can be obtained from the output power divided by the input power. The specific equation is as follows:

$$\eta_1 = \frac{p_o}{p_i} = \frac{F \times v}{p_i} \times 100\% \tag{8}$$

Among them, P_o is the output power, and P_i is the input power. F is the load force, and v is the speed under the load. The output power P_o can be obtained from the data in figure 11. The input power P_i can be tested with a power analyzer.

Figure 12 shows the relationship between efficiency and load calculated according to the equation (8). When the locking force is 2.5 N, and the load is 90 g, the maximum efficiency of the actuator is 1.29 %, and the output speed of the slider is 11.77 mm/s at this time. When the locking force is 3.5 N and the load is 120 g, the maximum efficiency of the prototype is 1.61 %, and the output speed of the slider is 10.63 mm/s at this time. When the locking force is 2.5 N and the load is 120 g, the maximum efficiency of the actuator is 1.39 %, and the output speed of the slider is 8.9 mm/s at this time. In the case that the load capacity of the prototype is hardly improved, the efficiency of the prototype is improved by increasing the speed of the prototype.

TABLE 4. Performance comparison with previous piezoelectric linear actuators.

Author	Material	Voltage (V)	Frequency (Hz)	Speed (mm/s)
[29]	Aluminium alloy	——	1400	3.75
[31]	65 Mn	80	3500	46.67
[32]	65 Mn	100	1000	18.60
[33]	AL 7075	150	2500	12.00
[38]	AL 7075	100	500	5.96
Proto-type	AL 7075	100	610	20.17

Table 4 compares the output speed characteristics of the piezoelectric actuator studied by previous researchers. It can be seen from the table that the flexible hinge mechanism proposed by the article based on the triangle amplification principle can improve the output speed of the actuator effectively at lower frequency.

V. CONCLUSION

To improve the output speed of the actuator at lower frequency, a stick-slip piezoelectric linear actuator based on triangular displacement amplification mechanism was proposed in this article. The designed triangular displacement amplification mechanism could realize high output speed at lower frequency. The main advantage of the proposed triangular displacement amplification mechanism is that not only the locking force during the driving process can be increased but also the displacement in the output direction can be amplified. The configuration and driving principle were illustrated. The design and simulation analysis of the triangular displacement amplification mechanism were discussed. A prototype was fabricated, and its output characteristics were tested. The experiment results indicated that

the maximum step efficiency is 97.9 % and the maximum output speed of the actuator was 20.17 mm/s when the locking force is 2.5 N. The article increased the output speed of the prototype by improving the step efficiency, thereby raising the efficiency of the prototype. The maximum value of the efficiency was about 1.61 % under the locking force of 3.5 N, the load of 120 g and the output speed of 10.63 mm/s. The experiment results confirmed that the triangular displacement amplification mechanism was effective for improving output speed at lower frequency. Further studies would be performed to improve its output performance of the proposed prototype.

REFERENCES

[1] S. Wang, W. Rong, L. Wang, H. Xie, L. Sun, and J. K. Mills, "A survey of piezoelectric actuators with long working stroke in recent years: Classifications, principles, connections and distinctions," *Mech. Syst. Signal Process.*, vol. 123, pp. 591–605, May 2019.

[2] Y. Zhang, K. Kiong Tan, and S. Huang, "Vision–servo system for automated cell injection," *IEEE Trans. Ind. Electron.*, vol. 56, no. 1, pp. 231–238, Jan. 2009.

[3] S. Wang, H. Arellano-Santoyo, P. A. Combs, and J. W. Shaevitz, "Actin-like cytoskeleton filaments fontribute to cell mechanics in bacteria," *Proc. Nat. Acad. Sci. USA*, vol. 107, no. 20, pp. 9182–9185, Oct. 2010.

[4] G. Schitter, K. J. Astrom, B. E. Demartini, P. J. Thurner, K. L. Turner, and P. K. Hansma, "Design and modeling of a high–speed AFM–scanner," *IEEE Trans. Control Syst. Technol.*, vol. 15, no. 5, pp. 906–915, Sep. 2007.

[5] C. Shi, D. K. Luu, Q. Yang, J. Liu, J. Chen, C. Ru, S. Xie, J. Luo, J. Ge, and Y. Sun, "Recent advances in nanorobotic manipulation inside scanning electron microscopes," *Microsyst. Nanoeng.*, vol. 2, no. 1, Dec. 2016, Art. no. 16024.

[6] S. Wang, H. Xu, Y. Wang, L. Kong, Z. Wang, S. Liu, J. Zhang, and H. Zhao, "Design and testing of a cryogenic indentation apparatus," *Rev. Sci. Instrum.*, vol. 90, no. 1, Jan. 2019, Art. no. 015117.

[7] K. Uchino, "Piezoelectric actuator renaissance," *Phase Transitions*, vol. 88, no. 3, pp. 342–355, Mar. 2015.

[8] M. Hunstig, "Piezoelectric inertia motors—A critical review of history, concepts, design, applications, and perspectives," *Actuators*, vol. 6, no. 1, pp. 7–42, Feb. 2017.

[9] T. Morita, "Miniature piezoelectric motors," *Sens. Actuators A, Phys.*, vol. 103, no. 3, pp. 291–300, Feb. 2003.

[10] Y.-T. Liu, T. Higuchi, and R.-F. Fung, "A novel precision positioning table utilizing impact force of spring-mounted piezoelectric actuator—Part II: Theoretical analysis," *Precis. Eng.*, vol. 27, no. 1, pp. 22–31, Jan. 2003.

[11] J. Li, R. Sedaghati, J. Dargahi, and D. Waechter, "Design and development of a new piezoelectric linear Inchworm actuator," *Mechatronics*, vol. 15, no. 6, pp. 651–681, Jul. 2005.

[12] J. Li, H. Zhao, X. Qu, H. Qu, X. Zhou, Z. Fan, Z. Ma, and H. Fu, "Development of a compact 2-DOF precision piezoelectric positioning platform based on inchworm principle," *Sens. Actuators A, Phys.*, vol. 222, pp. 87–95, Feb. 2015.

[13] L. Wang, W. Chen, J. Liu, J. Deng, and Y. Liu, "A review of recent studies on non-resonant piezoelectric actuators," *Mech. Syst. Signal Process.*, vol. 133, Nov. 2019, Art. no. 106254.

[14] Y. Liu, W. Chen, X. Yang, and J. Liu, "A rotary piezoelectric actuator using the third and fourth bending vibration modes," *IEEE Trans. Ind. Electron.*, vol. 61, no. 8, pp. 4366–4373, Aug. 2014.

[15] J. Li, H. Huang, and H. Zhao, "A piezoelectric–driven linear actuator by means of coupling motion," *IEEE Trans. Ind. Electron.*, vol. 65, no. 3, pp. 2458–2466, Mar. 2018.

[16] C.-F. Yang, S.-L. Jeng, and W.-H. Chieng, "Motion behavior of triangular waveform excitation input in an operating impact drive mechanism," *Sens. Actuators A, Phys.*, vol. 166, no. 1, pp. 66–77, Mar. 2011.

[17] Y. Peng, Y. Peng, X. Gu, J. Wang, and H. Yu, "A review of long range piezoelectric motors using frequency leveraged method," *Sens. Actuators A, Phys.*, vol. 235, pp. 240–255, Nov. 2015.

[18] X. Sun, W. Chen, J. Zhang, R. Zhou, and W. Chen, "A novel piezo-driven linear-rotary inchworm actuator," *Sens. Actuators A, Phys.*, vol. 224, pp. 78–86, Apr. 2015.

[19] S. Song, S. Shao, M. Xu, Y. Shao, Z. Tian, and B. Feng, "Piezoelectric inchworm rotary actuator with high driving torque and self-locking ability," *Sens. Actuators A, Phys.*, vol. 282, pp. 174–182, Oct. 2018.

[20] Y. Liu, X. Yang, W. Chen, and D. Xu, "A bonded–type piezoelectric actuator using the first and second bending vibration modes," *IEEE Trans. Ind. Electron.*, vol. 63, no. 3, pp. 1676–1683, Mar. 2016.

[21] M. Kuribayashi Kurosawa, O. Kodaira, Y. Tsuchitoi, and T. Higuchi, "Transducer for high speed and large thrust ultrasonic linear motor using two sandwich-type vibrators," *IEEE Trans. Ultrason., Ferroelectr., Freq. Control*, vol. 45, no. 5, pp. 1188–1195, Sep. 1998.

[22] L. Wang, J. Liu, S. Chen, K. Li, and Y. Liu, "Design and fabrication of a high-speed linear piezoelectric actuator with nanometer resolution using a cantilever transducer," *Smart Mater. Struct.*, vol. 28, no. 5, May 2019, Art. no. 055035.

[23] Y. Liu, W. Chen, J. Liu, and X. Yang, "A high–power linear ultrasonic motor using bending vibration transducer," *IEEE Trans. Ind. Electron.*, vol. 60, no. 11, pp. 5160–5166, Nov. 2013.

[24] Z. M. Zhang, Q. An, J. W. Li, and W. J. Zhang, "Piezoelectric friction–inertia actuator—A critical review and future perspective," *Int. J. Adv. Manuf. Technol.*, vol. 62, nos. 5–8, pp. 669–685, Sep. 2012.

[25] D. Kang, M. G. Lee, and D. Gweon, "Development of compact high precision linear piezoelectric stepping positioner with nanometer accuracy and large travel range," *Rev. Sci. Instrum.*, vol. 78, no. 7, Jul. 2007, Art. no. 075112.

[26] Y. Wang, J. Zhu, M. Pang, J. Luo, S. Xie, M. Liu, L. Sun, C. Zhou, M. Tan, J. Ge, Y. Sun, and C. Ru, "A Stick–Slip Positioning Stage Robust to Load Variations," *IEEE/ASME Trans. Mechatronics*, vol. 21, no. 4, pp. 2165–2173, Aug. 2016.

[27] F. Dubois, C. Belly, A. Saulot, and Y. Berthier, "Stick-slip in stepping piezoelectric Inertia Drive Motors—Mechanism impact on a rubbing contact," *Tribology Int.*, vol. 100, pp. 371–379, Aug. 2016.

[28] M. Hunstig, T. Hemsel, and W. Sextro, "Stick–slip and slip–slip operation of piezoelectric inertia drives. Part I: Ideal excitation," *Sens. Actuators A, Phys.*, vol. 200, pp. 90–100, Oct. 2013.

[29] J. Wei, S. Fatikow, X. Zhang, and O. C. Haenssler, "Design and experimental evaluation of a compliant mechanism-based stepping-motion actuator with multi-mode," *Smart Mater. Struct.*, vol. 27, no. 10, Oct. 2018, Art. no. 105014.

[30] J. Wang, J. Li, Z. Xu, S. Wang, Z. Wang, B. Xu, Y. Sun, S. Liu, and H. Zhao, "Design, analysis, experiments and kinetic model of a high step efficiency piezoelectric actuator," *Mechatronics*, vol. 59, pp. 61–68, May 2019.

[31] Y. Zhang, Y. Peng, Z. Sun, and H. Yu, "A novel stick–slip piezoelectric actuator based on a triangular compliant driving mechanism," *IEEE Trans. Ind. Electron.*, vol. 66, no. 7, pp. 5374–5382, Jul. 2019.

[32] Y. Zhang, M. Wang, Y. Fan, T.-F. Lu, Y. Cheng, and Y. Peng, "Improving load capacity of stick-slip actuators in both driving directions via a shared driving foot," *Smart Mater. Struct.*, vol. 28, no. 6, Jun. 2019, Art. no. 065004.

[33] B. W. Zhong, J. Zhu, Z. Q. Jin, H. D. He, Z. H. Wang, and L. N. Sun, "A large thrust trans-scale precision positioning stage based on the inertial stick-slip driving," *Microsyst. Technol.*, vol. 25, no. 10, pp. 3713–3721, Oct. 2019.

[34] Q. S. Zhang, X. B. Chen, Q. Yang, and W. J. Zhang, "Development and characterization of a novel piezoelectric-driven stick-slip actuator with anisotropic-friction surfaces," *Int. J. Adv. Manuf. Technol.*, vol. 61, nos. 9–12, pp. 1029–1034, Aug. 2012.

[35] Y. Li, H. Li, T. Cheng, X. Lu, H. Zhao, and P. Chen, "Note: Lever-type bidirectional stick-slip piezoelectric actuator with flexible hinge," *Rev. Sci. Instrum.*, vol. 89, no. 8, Aug. 2018, Art. no. 086101.

[36] T. Cheng, H. Li, M. He, H. Zhao, X. Lu, and H. Gao, "Investigation on driving characteristics of a piezoelectric stick–slip actuator based on resonant/off-resonant hybrid excitation," *Smart Mater. Struct.*, vol. 26, no. 3, Mar. 2017, Art. no. 035042.

[37] Z. Guo, Y. Tian, D. Zhang, T. Wang, and M. Wu, "A novel stick-slip based linear actuator using bi-directional motion of micropositioner," *Mech. Syst. Signal Process.*, vol. 128, pp. 37–49, Aug. 2019.

[38] T. Cheng, M. He, H. Li, X. Lu, H. Zhao, and H. Gao, "A novel trapezoid–type stick–slip piezoelectric linear actuator using right circular flexure hinge mechanism," *IEEE Trans. Ind. Electron.*, vol. 64, no. 7, pp. 5545–5552, Jul. 2017.

XIAOHUI LU was born in Jilin, China. She received the B.S. degree in mathematics and applied mathematics from Beihua University, Jilin, in 2004, the M.S. degree in operational research and cybernetics from the Lanzhou University of Technology, Lanzhou, China, in 2007, and the Ph.D. degree in control theory and application from Jilin University, Changchun, China, in 2013. She was a Visiting Scholar with the School of College of Engineering, The Ohio State University, under the supervision of J. Wang, from 2017 to 2018. Her current research interests include vehicle powertrain control, model predictive control, data-driven control, and triboelectric nanogenerators.

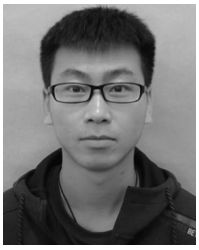

QIANG GAO was born in Shanxi, China, in 1994. He received the B.S. degree from the Luoyang Institute of Science and Technology, Luoyang, China, in 2018. He is currently pursuing the M.S. degree in mechanical engineering with the Changchun University of Technology. His research interests include piezoelectric actuators and triboelectric nanogenerators.

YIKANG LI was born in Jilin, China, in 1994. He received the B.S. degree from the Changchun University of Technology, Changchun, China, in 2017, where he is currently pursuing the M.S. degree with the Department of Mechanical Engineering. His research interests include piezoelectric actuators and smart materials and structures.

YANG YU was born in Jilin, China, in 1995. He received the B.S. degree from the Changchun University of Technology, Changchun, China, in 2018, where he is currently pursuing the M.S. degree in mechanical engineering. His research interests include friction drive mechanism and piezoelectric energy harvesting.

XIAOSONG ZHANG was born in Sichuan, China, in 1996. He received the B.S. degree from the Changchun University of Technology, Changchun, China, in 2019. His research interest includes piezoelectric actuators.

GUANGDA QIAO was born in Shandong, China, in 1997. He received the B.S. degree from the Changchun University of Technology, Changchun, China, in 2019, where he is currently pursuing the M.E. degree. His research interest includes piezoelectric actuators.

TINGHAI CHENG received the B.S., M.S., and Ph.D. degrees from the Harbin Institute of Technology, in 2006, 2008, and 2013, respectively. He was a Visiting Scholar with the School of Materials Science and Engineering, Georgia Institute of Technology, from 2017 to 2018. He is currently a Professor with the School of Mechatronic Engineering, Changchun University of Technology. His research interests are piezoelectric actuators, piezoelectric energy harvester, and triboelectric nanogenerators.